ACS Biomaterials SCIENCE & ENGINEERING

Article

pubs.acs.org/journal/abseba

De Novo Engineering of Solid-State Metalloproteins Using Recombinant Coiled-Coil Silk

Trevor D. Rapson,*[,†] Tara D. Sutherland,*[,†] Jeffrey S. Church,[‡] Holly E. Trueman,[†] Helen Dacres,[§] and Stephen C. Trowell[†]

[†]CSIRO, Black Mountain, Canberra, ACT 2601, Australia

[‡]CSIRO, Waurn Ponds, Geelong, Victoria 3216, Australia

[§]CSIRO Werribee, Victoria 3030, Australia

Supporting Information

ABSTRACT: To achieve the sophisticated chemistry required for life, nature uses metal containing proteins (metalloproteins). However, despite intensive research efforts, very few of these metalloproteins have been exploited for biotechnological applications. One major limiting factor is the poor stability of these proteins when they are removed from their cellular environment. To produce stable metalloproteins, we have developed an engineering strategy that uses structural proteins which can be fabricated into a number of different solid-state materials. Here we demonstrate that a recombinant silk protein (AmelF3 − *Apis mellifera* Fibroin 3) binds heme and other metal macrocycles in a manner reminiscent of naturally occurring metalloproteins, whereby an amino acid coordinates directly to the metal center. Our strategy affords design at four different levels: the metal center, the organic macrocycle, the protein scaffold, and the material format structure. The solid-state metalloproteins produced remained functional when stored at room temperature for over one year.

KEYWORDS: *heme, recombinant silk, biosensors, biocatalysis, industrial biotechnology*

INTRODUCTION

The engineering of metalloprotein mimics is attracting increasing interest both as a route to understanding natural protein structure−function and for a range of biotechnological applications.[1−3] The heme protein family is of particular interest because of the diversity of chemical functions accessible through the interaction of the iron heme metal center with a variable protein scaffold (Figure 1a).[4−6] The ability to harness the functional properties of heme proteins within a solid-state material affords a number of potential practical advantages, such as stability and recyclability, for heterogeneous biocatalysts and biosensors.[7]

The minimum structural requirements to mimic native metalloprotein function has been investigated using de novo engineering of metal binding sites into α-helical peptides that form bundles in solution (Figure 1a).[2,6,9] This approach has produced artificial molecules capable of oxygen-binding,[10] light harvesting,[11] transmembrane transport[12] and catalysis.[5,13−15] In this work we sought to transfer the insights gained by de novo engineering from the solution-state to solid-state materials. In particular, we have focused on the use of transgenic honeybee silk (AmelF3) as a new protein scaffold for metalloprotein engineering.[16]

A number of recent reports have described the engineering of structural proteins to bind metals.[17−21] This approach has allowed new functions to be introduced into structural materials. For example, the addition of short silver binding

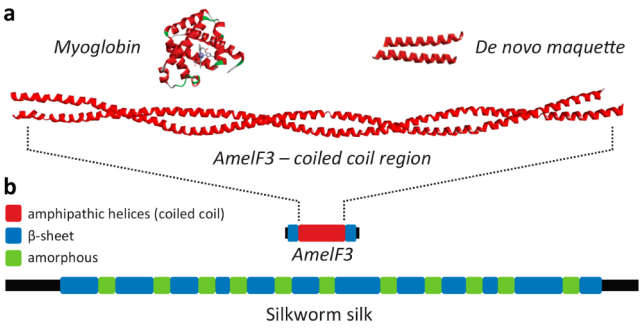

Figure 1. (a) Comparison between naturally occurring heme protein structures and engineering scaffolds. Cartoon structures of a common heme protein with an α-helical structure (myoglobin−pdb, 2VIK), the de novo maquette scaffolds used to produce engineered metalloproteins (pdb, 1M3W)[8] and the predicted coiled-coil structure of recombinant honeybee silk (AmelF3) modeled from tropomyosin (pdb, 1C1G). (b) Comparison of the molecular structure of AmelF3 (*Apis mellifera* Fibron 3−30 kDa) and silkworm silk (heavy fibron ∼250 kDa). The β-sheeted regions of silkworm silk are made up of repetitive regions containing (i) GAGAGS, (ii) GAGAGY and/or AGAGVGY, (iii) similar to i, except for the presence of an AAS motif.

Received: June 3, 2015
Accepted: September 23, 2015
Published: September 23, 2015

DOI: 10.1021/acsbiomaterials.5b00239
ACS Biomater. Sci. Eng. 2015, 1, 1114−1120

peptides to spider silk produced a chimeric protein which could be cast into films with antimicrobial properties.[22] Through covalent attachment of titanium binding peptides to silkworm silk, enhanced cellular adhesion to titanium-based implants was achieved.[17] Krishnaji and Kaplan developed a chimera between a uranium peptide recognition motif and spider silk, which has potential applications in the area of bioremediation.[18] Although in these examples the structural proteins can be fabricated into solid-state materials, the goal was not to mimic metalloprotein function but rather produce a material capable of binding metals such as uranium for bioremediation,[18] or for releasing metal ions, as in the case for antimicrobial activity.[22] In contrast, here we sought to control the reactivity of the metal center via direct interaction with the protein scaffold, to carry out functions such as catalysis.[23]

Honeybee larvae spin silken cocoons that contribute to the mechanical and thermal stability of the hive.[24] The honeybee silk proteins, unlike silkworm and spider silk, adopt a molecular structure with a large central coiled coil domain (~210 $\alpha\alpha$) with short (20−50 $\alpha\alpha$) β-sheeted regions at the N and C termini (Figure 1b).[25,26] This coiled coil structure is similar to the α-helical de novo maquettes (Figure 1a) successfully used by other groups to engineer metalloprotein mimics. While natural honeybee silk is made up of four fibrous proteins,[27] a single fibroin of honeybee silk (*Apis mellifera* Fibron 3, AmelF3) can be fabricated into various solid-state materials including fibers,[28,29] sponges,[30] and films.[31] Importantly, AmelF3 can be produced at high levels (>2g/L) in recombinant systems[16] making commercial production viable. The extensive natural variation found among honeybee silk homologues[32] suggests that the AmelF3 fibroin's amino acid sequence can be substantially varied to insert or modify metal and macrocycle binding sites without comprising the proteins ability to be fabricated into material forms.

In this work, we describe the use of AmelF3 as an engineering scaffold to mimic naturally evolved heme-containing proteins. Heme proteins are attractive targets for de novo engineering,[5,9,33] given the diverse functions they perform using a common iron porphyrin ring. One of the principal ways that the reactivity of naturally occurring heme proteins is controlled is through direct coordination of the iron by an amino acid residue.[34] The importance of direct interaction between the protein scaffold environment and metal center to metalloprotein function has become increasingly clear.[23,35−37] Our immediate goal was to achieve both binding and direct coordination of heme cofactors to AmelF3. If coordination can be achieved, this would allow further tuning of reactivity through varying the identities of the coordinating residue and the metal macrocycle.

EXPERIMENTAL SECTION

Materials. All standard chemicals used were purchased from Sigma-Aldrich (St Louis, MO) unless stated otherwise. Heme *b*, copper and cobalt protoporphyrin IX and tetrasulfonate zinc phthalocyanine were purchased from Frontier Scientific (Logan, UT). Cobyrinic acid heptamethyl ester was purchased from Sigma-Aldrich. UV/vis absorption measurements were carried out on a SpectraMax M2 plate reader.

Silk Protein Preparation. Recombinant honeybee silk protein, AmelF3, was produced by fermentation in *Escherichia coli* as described by Weisman et al.[16] Briefly, purified inclusion bodies were solubilized by addition of equal dry weight sodium dodecyl sulfate (SDS) from 1−10% solutions as required. The majority of the detergent was then removed by centrifugation after addition of 300 mM KCl which led to its potassium-induced precipitation. This treatment generated high-purity AmelF3 solutions containing approximately 0.3% SDS weight/volume. The AmelF3 solution was dialyzed against 15% polyethylene glycol (PEG) to generate a solution containing 3.6% protein and 0.3% SDS.

Metal Macrocycle Solution Preparation. Heme *b* (iron protoporphyrin IX), cobalt protoporphyrin IX and copper protoporphyrin IX were initially dissolved in a minimal amount of 0.1 M NaOH (~1 mL) and made up in 70% methanol to give a final volume of 10 mL. Other macrocycles such as cobyrinic acid heptamethyl ester and tetrasulfonate zinc phthalocyanine were dissolved directly in 70% methanol. Concentrations of ~0.05 mg/mL were used for all macrocycles.

Metal-Functionalized Silk Material Preparation. AmelF3 silk protein sponges were generated as follows; AmelF3 protein solution was poured into silicone rubber molds (14 × 5 × 6 mm; RL060, ProSciTech, QLD), frozen at −20 °C overnight, and placed in a freeze-dryer (FD355DMP, FTS Systems) for 24 h to generate sponges with typical dimensions of 12.6 × 4.5 × 5.4 mm. The silk sponges were stored in sealed plastic bags at room temperature until use. Silkworm silk sponges were a gift from Prof David Kaplan.

Heme *b* (or other macrocycles) could be added to the honeybee silk or silkworm silk sponges by adding solutions of the macrocycle (in 70% methanol) dropwise to the sponge (~10 mg protein). Aqueous 70% methanol was used as the solvent for AmelF3 materials as they are not soluble in 70% methanol. An alternative method of preparing silk-heme sponges was to place a freeze-dried sponge into a 10 mL solution of macrocycle and allow the sponge to absorb the solution until fully saturated. The sponge was washed 3 times with 70% aqueous methanol (10 mL per wash), air-dried and stored at room temperature.

Silk films were prepared by either codrying heme and silk protein, or by leaching heme into preformed films. Codrying involved dissolving the equivalent of 1 mg of heme *b* with 10 mg of recombinant honeybee silk sponges in 0.5 mL of hexafluoroisopropanol (HFIP) overnight at room temperature. The solution was aliquoted into either a cuvette or a 24-well plate, air-dried at room temperature and stored until required. The dried film was soaked overnight in 70% methanol to make the film insoluble in water. To add heme *b* (or an other metal macrocycle) to a preformed film, the film was first prepared by dissolving a sponge in Milli-Q water (~10 mg silk in 1 mL of water) and then a drop (~100 uL) of the solution was air-dried on a plastic surface to generate a disk film. The film was soaked in 1 mL of the macrocycle solution (0.05 mg/mL) for 48 h followed by washing with 70% methanol to remove unbound heme.

Substituting Tyrosine in AmelF3. Site-directed mutagenesis was carried out using Pfx50 DNA polymerase from Invitrogen (Carlsbad, CA), with overlapping primers to introduce the desired mutation (see the Supporting Information) according to the manufacturer's instructions. The template plasmid was removed by Dpn1 digestion following PCR amplification. Sequencing was carried out at the Micromon sequence facility (Monash University, Australia) using T7 primers. Try76Ala and Tyr76His substituted protein was expressed and purified as described for the unmodified silk protein.

Nitric Oxide Binding Assay. Heme *b*-silk films were covered with 50 mM phosphate buffer (pH 7) and reduced by the addition of ~10 μL sodium dithionite (100 mM) in phosphate buffer (pH 7). Diethylamine 2-nitrosohydrazine sodium hydrate (NONOate) was dissolved in 50 mM phosphate (pH 7) to generate 1.5 mol equivalent of dissolved NO. Aliquots of the diethylamine NONOate solution was added incrementally to a dithionite reduced film under argon gas. Changes in the UV−vis spectrum were monitored to determine redox states and measure NO binding. The experiment was carried out in triplicate using separate films, allowing standard deviations to be calculated for each point.

Peroxidase Assay. The protocol outlined by the Worthington Biochemical Corporation at http://www.worthington-biochem.com/hpo/assay.html was adapted as follows. A solution of 1.7 mM H_2O_2 (prepared from a 30% solution purchase from Sigma (St Louis, MO) was mixed with a solution of 2.5 mM 4-aminoantipyrine (JT Baker

DOI: 10.1021/acsbiomaterials.5b00239
ACS Biomater. Sci. Eng. 2015, 1, 1114−1120

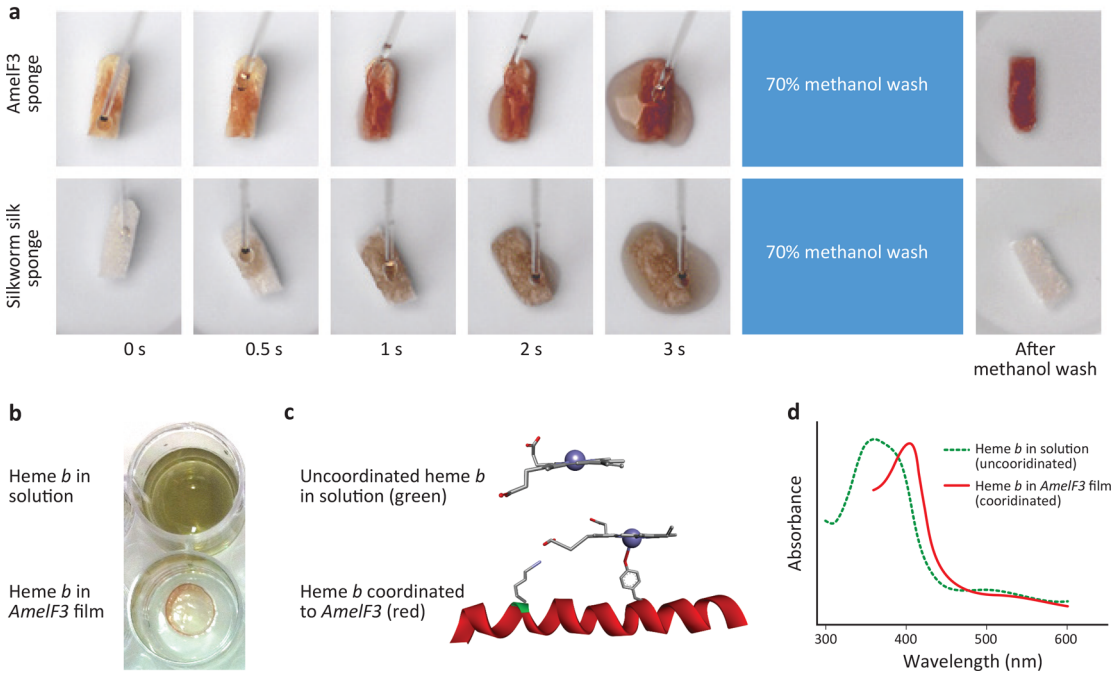

Figure 2. Production and optical properties of a solid-state biomimetic metalloprotein. (a) Evidence for specific binding and coordination of heme *b* within honeybee silk sponges. A solution of heme *b* was added to a honeybee silk sponge (top panel) and a silkworm sponge (bottom panel). The sponges were then washed with 70% methanol. (b) Heme *b* in 70% methanol (top) could be diffused into a preformed film to yield a heme *b* containing silk film (bottom). (c) Cartoon representation of heme *b* binding and coordinating to AmelF3 giving rise to the color change in the heme *b* cofactor from green, uncoordinated, to red, coordinated. (d) UV−visible spectrum of a heme *b*-silk film compared to that of heme *b* in aqueous solution. A video of the addition of heme *b* solutions to AmelF3 and silkworm silk is provided in the Supporting Information.

(Center Valley, PA)) and 170 mM phenol (Sigma (St Louis, MO)) in a 1:0.9 ratio. Heme *b*-silk sponges were added to this solution and absorbance at 510 nm was monitored over time. In this assay Fe^{3+} is oxidized by hydrogen peroxide and then reduced by 4-aminoantipyrine (hydrogen donor), which in turn oxidatively couples to phenol to form a pink colored quinone.

Raman Spectroscopy. Raman spectra were obtained using a Renishaw inVia confocal microscope system with 754 nm excitation from a Renishaw HPNIR diode laser through a ×50 (0.75 na) objective. Incident laser power, as measured using an Ophir Nova power meter fitted with a photodiode head, was 4.93 mW for the silk films and 0.66 mW for the heme *b* powder. Films were held on a mirrored backing. The powder was compressed into a 2 mm cavity cell. A coaxial backscatter geometry was employed. Spectra were collected over the range of 100 to 1900 cm^{-1} and averaged over at least 4 scans, each with an accumulation time of 20 s. For the films, six spectra collected from different sample areas were averaged to produce the final spectrum. Raman shifts were calibrated using the 520 cm^{-1} line of a silicon wafer. The spectral resolution was approximately 1 cm^{-1}.

Fourier Transform Infrared Spectroscopy. Infrared attenuated total reflectance (ATR) spectra were obtained using a PerkinElmer (Beaconsfield, UK) Spectrum 100 Fourier transform infrared (FTIR) spectrometer equipped with a universal micro-ATR accessory and purged with liquid nitrogen boil off. Spectra were collected at a resolution of 4 cm^{-1} by coaveraging a minimum of 16 interferograms. Manipulation of spectral data was carried out using Grams AI v 9.1 software (Thermo Fischer Scientific, USA).

RESULTS AND DISCUSSION

Initially, we tested the binding of the most commonly occurring heme cofactor, heme *b*, to freeze-dried honeybee silk sponges. Given the coiled coil structure of AmelF3 and the large number of positively charged amino acid residues such as lysine and arginine, we expected that heme *b* would bind weakly to the unmodified honeybee silk protein. However, when a honeybee silk sponge was exposed to heme *b* solutions, which are green, the sponge immediately turned red (Figure 2a, top panel), indicating a change in the coordination of the iron metal center within the heme group. Furthermore, the binding of heme *b* to honeybee silk was found to be strong; the cofactor could not be removed by washing the heme *b*-silk sponges with aqueous solutions, 70% methanol in water (Figure 2a−top panel), 0.1 M hydrochloric acid or 0.1 M sodium hydroxide and organic solvents such as chloroform.

In contrast, when heme *b* was added to sponges composed of silkworm (*Bombyx mori*) cocoon silk proteins, the green heme *b* solution was absorbed by the sponge but was readily washed out with 70% methanol (Figure 2a, bottom panel, Video S1).

Our results clearly indicate that heme *b* was able to bind to AmelF3 but not to silkworm silk sponges. The majority of naturally occurring heme proteins such as the globins and cytochromes have an α-helical structure (e.g., myoglobin Figure 1a). In these proteins, the heme cofactor is held within the protein through a combination of hydrophobic packing, ionic or hydrogen bonding between the heme propionate groups and charged or polar amino acid residues such as arginine, tyrosine or serine.[3,38] It is therefore likely that the coiled-coil structure of AmelF3 assists with the binding of heme *b* by providing a hydrophobic environment. Furthermore, AmelF3 is rich in charged residues such as lysine (7.5%) or hydrogen bond donors such as serine (11.3%), which can interact with the propionate groups of heme *b*.

In addition to the strong binding of heme *b* by AmelF3, the color change from green to red noted upon the addition of heme *b* to honeybee silk sponges (Figure 2a) indicates a change in the coordination of the iron metal center within the heme group. To investigate this further, we analyzed the UV−vis

DOI: 10.1021/acsbiomaterials.5b00239
ACS Biomater. Sci. Eng. 2015, 1, 1114−1120

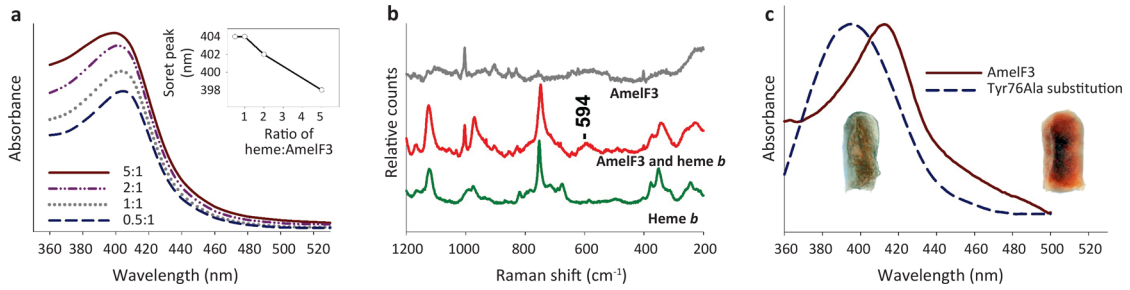

Figure 3. A tyrosine in honeybee silk specifically coordinates to heme *b*. (a) UV−vis spectra of honeybee silk films containing varying amounts of heme *b*. Inset shows the change in the position of the Soret peak with differing molar ratios of heme *b*. (b) Raman spectra from honeybee silk (gray trace) heme *b*-silk (red trace) and heme *b* powder (green trace) excited at 785 nm. (c) UV−vis spectra of films made from Tyr76Ala silk compared with unmodified honeybee silk films. Inset show photos of unmodified silk sponge (red) and Tyr76Ala sponge (green) following washing with 70% methanol.

spectra of heme *b* diffused into preformed transparent films (Figure 2b−d). Heme proteins have a characteristic Soret peak at ∼400 nm, which is sensitive to changes in the coordination of the iron heme atom. In the case of iron porphyrins, such as heme *b*, broad Soret peaks below 400 nm indicate that the iron is coordinated to the porphyrin ring (4-coordinate) but not the protein. When the heme group is also coordinated to an amino acid in the protein, the Soret band red shifts above 400 nm and sharpens, as a five-coordinate iron center is generated.[39] The UV−vis spectrum from the honeybee silk-heme *b* films show a sharp Soret peak at 404 nm (Figure 2d) confirming that the iron heme center is coordinated to the honeybee silk protein (AmelF3). These results indicate that AmelF3 silk materials bind and coordinate heme *b* in a manner resembling naturally occurring heme proteins.

Given that we observed that heme *b* both binds and coordinates to AmelF3, we sought to determine the effect of adding heme *b* on the molecular structure of AmelF3 in the form of a film. Fourier transform infrared spectroscopy (FTIR) allows the secondary structure of protein materials to be investigated using the amide I and III modes.[40,41] The FTIR spectra of both dried films and those stabilized with 70% methanol were measured to compare films with and without heme *b* (Figure S1). No conformational differences were detected due to the addition of heme *b* (Figure S1).

As previously described for dried AmelF3 materials,[16] both spectra of the dried films exhibit amide I peak maxima at 1646 cm^{-1}, which is consistent with that expected for a dominant coiled coil structure. A weaker low wavenumber shoulder was also observed, indicative of a minor amount of β-sheet structure. The amide III region exhibits peaks at both 1304 cm^{-1} (coiled coil) and 1235 cm^{-1} (β-sheet).

Following stabilization with 70% methanol, the spectra were similar to that reported previously,[16,30] with amide I peak maxima at 1644 and 1626 cm^{-1}. This is consistent with increased β-sheet structure (1626 cm^{-1}). We have previously determined by infrared spectroscopy that methanol treatment results in a 10% decrease in coiled coil conformation with a corresponding increase in β-sheet content.[16]

To allow further engineering options it was important to understand exactly which residues of AmelF3 where coordinating to the iron center of heme *b*. AmelF3 does not contain any of the coordinating residues typically found in natural heme proteins, such as histidine, cysteine, or methionine (Figure S2). Therefore, to identify the coordinating amino residue, we investigated the stoichiometry of heme binding and coordination. By codrying heme and protein solutions, rather than diffusing heme *b* into preformed films, we were able to prepare films with varying ratios of heme *b* to silk protein. At low heme loadings (heme:protein molar ratios of 1:1 and 1:2), a sharp Soret peak was observed at 404 nm, indicating that the majority of the heme was coordinated (Figure 3a). As the ratio of heme *b* to protein was increased, the Soret peak broadened and shifted to lower wavelengths, indicating an increase in the amount of uncoordinated heme. This finding suggests that a single site within each silk monomer is responsible for heme coordination.

Raman spectroscopy was used to measure stretching frequencies between the iron center and the coordinating ligand, which are indicative of the identity of the ligand.[42] The Raman spectrum of the silk-heme film, excited at 785 nm, showed a broad peak centered at 594 cm^{-1} (red trace, Figure 3b). Heme proteins that have a tyrosine coordinating ligand show similar Fe-Tyr stretches.[43,44] AmelF3 contains a single tyrosine residue (Tyr76) located in the core of the coiled coil region. To test whether Tyr76 is the coordinating ligand, we replaced Tyr76 with alanine using site directed mutagenesis. When heme *b* was added to sponges formed from Try76Ala modified protein, the sponge did not become red (Figure 3c, inset) suggesting that no coordination change to the heme cofactor was occurring. Furthermore, the UV−vis spectrum of transparent films generated from the Tyr76Ala substituted protein had a broad Soret peak at 395 nm indicating that the coordination observed in unmodified honeybee silk had been reversed by this single amino acid substitution (Figure 3c). Nevertheless, the uncoordinated (green) heme *b* could not be washed out of the sponge, indicating that the cofactor still bound to the Tyr76Ala silk, even though the iron center was not coordinated to the silk (Figure 3c, inset). This binding is most likely mediated via interactions between the propionate group of heme *b* and charged or polar residues of AmelF3 and the hydrophobic core of the coiled-coil domain. Although silkworm silk has over 4% tyrosine residues, none of these residues coordinates, or binds, heme *b* in the manner observed for AmelF3 (Figure 2). This result suggests that in addition to the presence of a coordinating residue, the molecular architecture of AmelF3 plays an important role in both the binding and coordination of heme *b*.

To further demonstrate that the binding site could be modified, we used site directed mutagenesis to change the coordinating tyrosine residue to a histidine, the residue most commonly found in natural heme proteins.[4,45] A Tyr76His modification induced a red shift of the Soret peak to 410 nm in films generated from this recombinant AmelF3 material (Figure

DOI: 10.1021/acsbiomaterials.5b00239
ACS Biomater. Sci. Eng. 2015, 1, 1114−1120

S3), consistent with coordination of histidine to the metal center.[39,46]

Uncoordinated heme and heme-like cofactors have been widely used in biomimetic chemistry. Their lack of coordination, however, has limited their usefulness.[7] Using AmelF3, as described here, we can vary the coordination of the heme center, allowing more precise control over the functional properties of the metalloproteins.

To demonstrate the catalytic potential of solid-state metalloproteins, we engineered a heterogeneous catalyst based on a heme *b* silk sponge. Heme peroxidases catalyze the breakdown of phenol derivatives, one of the largest groups of pollutants in industrial effluents.[47−49] The catalytic mechanism involves peroxidase oxidation by hydrogen peroxide followed by reduction of the peroxidase by a substrate such as a phenol or aromatic amine (Figure 4a). We tested the catalytic activity

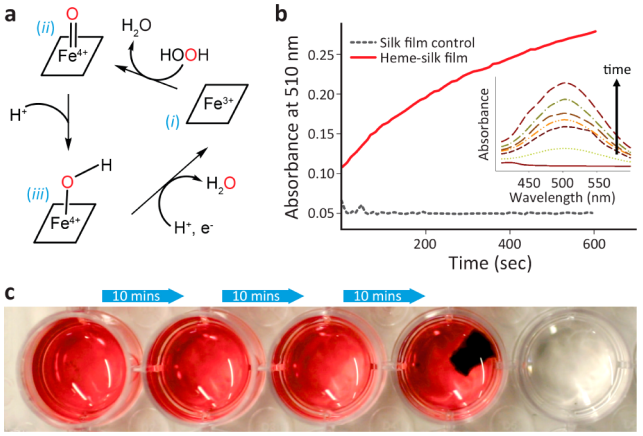

Figure 4. Demonstration of catalytic activity by heme *b*-AmelF3 materials. (a) The catalytic mechanism of heme *b*-silk peroxidase activity. 4-aminoantipyrine acts as the substrate reducing the heme center. (b) Time course of phenol oxidation by heme *b*-AmelF film. Coupling of phenol to 4 amino-antipyrine gives a colored quinone. Inset shows the change in the solution UV/vis spectrum over time. (c) A heme-AmelF3 sponge was transferred through a series of wells containing 4-aminoantipyrine (1.1 mM), phenol (80 mM) and H_2O_2 (0.9 mM). The rightmost well contains a solution to which the sponge has not yet been added. The second well from the right contains the sponge.

of heme *b*-silk materials using the oxidative coupling of phenol with 4-aminoantipyrine to produce a pink quinone with λ_{max} = 510 nm (Figure 4b, Figure S4). The heme *b*-silk sponges readily catalyzed the coupling of phenol to 4-aminoantipyrine in aqueous media. Furthermore, the sponges were recoverable, they could be reused at least six times (Figure 4c) and remained functional if stored dry at room temperature for over one year.

As a second example of the properties of solid-state metalloproteins we used a heme *b*-silk film as a nitric oxide sensor. The films were sensitive to nitric oxide at submicromolar concentrations and the binding was reversible (Figure S5). In addition, the sensing property was retained in films stored dry at ambient humidity and room temperature for more than a year (Figure 5). Poor stability at room temperature of many biologically derived materials is one of the factors that has prevented the transition of metalloproteins from the research laboratory to commercial applications. This work demonstrated that stable metalloprotein biosensor materials

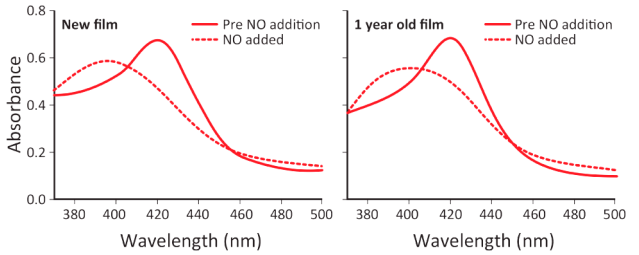

Figure 5. Heme *b*-silk films as a stable biosensor. The UV/vis spectra of a reduced heme *b*-silk film before (solid line) and after (dashed line) the addition of nitric oxide. Left panel: freshly prepared film. Right panel: nitric oxide binding of the same film after storage for 1 year at ambient conditions.

can be produced through the use of a stable protein as the engineering scaffold.

We have demonstrated the ability to produced heme *b*-AmelF3 materials in different formats such as sponges and films. The reactivity of the iron heme center can be altered through varying the coordinating ligand from AmelF3. To broaden our engineering options, we extended our survey beyond heme cofactors to other metal macrocycles. Biological systems incorporate a range of nonheme metal macrocycles in proteins, such as the magnesium chlorophylls in Photosystem II[50] and the cobalt corrins in Vitamin B12.[51,52] Inspired by nature's metal cofactors, synthetic chemists have produced a range of compounds such as the metallophthalocyanines that are used in dye-sensitized solar cells[53,54] and photodynamic therapy.[55] Varying the metal center and organic cofactor allows additional avenues of engineering to produce solid-state materials with different functional properties (Figure 6a).

We therefore sought to determine if AmelF3 materials could be engineered to incorporate other cofactors besides iron heme. We were readily able to replace the iron in heme with copper or cobalt (Figure 6b), which can alter functional properties. For example, cobalt-substituted hemes have been used as selective nitric oxide sensors.[56] In addition to hemes, other organic macrocycles, such as corrin and phthalocyanine rings (Figure S6), bind to AmelF3 materials (Figure 6b). The use of the versatile family of metallophthalocyanines in catalytic applications has been limited by their poor solubility in water.[57] The ability to produce heterogeneous catalysts with poorly water-soluble metal macrocycles such as heme *b* and metallophthalocyanines provides an avenue to accessing their catalytic properties within aqueous systems. We will investigate the properties of these materials in future work.

CONCLUSIONS

In this work, we demonstrate the engineering of a solid-state metalloprotein material that can be precisely tuned for a variety of different functions at four different levels; namely the metal center, the organic macrocycle, the protein scaffold and the material structure (Figure 6). These solid-state metalloproteins are remarkably stable and reusable. The ability to produce large quantities, the ease of manipulating the protein sequence, and the long-term stability of materials made from this protein make recombinant honeybee silk a promising template for de novo engineering of a wide range of biomimetic metalloprotein materials with diverse functional properties.

DOI: 10.1021/acsbiomaterials.5b00239
ACS Biomater. Sci. Eng. 2015, 1, 1114−1120

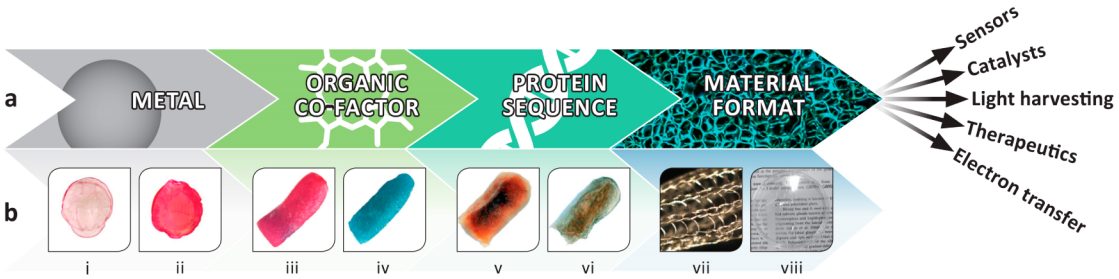

Figure 6. Engineering options for the development of solid-state metalloproteins. (a) Schematic representation of the four different levels of engineering control available to produce solid-state materials for a diverse range of applications. (b) Examples of solid-state materials developed: AmelF3 films with (i) copper protoporphryin IX and (ii) cobalt protoporphyrin IX. AmelF3 sponges with (iii) cobyrinic acid heptamethyl ester and (iv) tetrasulfonate zinc phthalocyanine (molecular structures shown in Figure S6). AmelF3 sponges with heme *b*: (v) unmodified, (vi) Y76A substitution. In all cases, solid-state materials were thoroughly washed with 70% methanol to remove unbound macrocycle. (vii) AmelF3 fibers (knitted), (viii) AmelF3 transparent films (no metal cofactors added).

■ ASSOCIATED CONTENT

Supporting Information

The Supporting Information is available free of charge on the ACS Publications website at DOI: 10.1021/acsbiomaterials.5b00239.

Mutagenesis primers, FTIR spectra of silk films with and without heme-*b*, AmelF3 sequences, and additional data. W(PDF)

Link to dropbox video demonstrating the production of heme-silk sponges and how heme does not bind to B.mori silk (PDF/MP4)

■ AUTHOR INFORMATION

Corresponding Authors

*E-mail: trevor.rapson@csiro.au.

*E-mail: tara.sutherland@csiro.au.

Author Contributions

T.D.R. and T.D.S contributed equally to this work.

Notes

The authors declare no competing financial interest.

■ ACKNOWLEDGMENTS

We thank Dr Gunjan Pandey for his assistance in photographing the silk sponges, Ms Andrea Woodhead for her assistance in collecting the Raman spectra, Dr Alagacone Sriskantha for preparing honeybee silk protein samples, Dr Peter Campbell for his assistance in the preparation of this manuscript and Dr Andrew Warden for discussions prior to publication. Samples of silkworm silk were a gift from Prof David Kaplan.

■ REFERENCES

(1) Lu, Y.; Yeung, N.; Sieracki, N.; Marshall, N. M. Design of functional metalloproteins. *Nature* **2009**, *460*, 855−862.

(2) Yu, F.; Cangelosi, V. M.; Zastrow, M. L.; Tegoni, M.; Plegaria, J. S.; Tebo, A. G.; Mocny, C. S.; Ruckthong, L.; Qayyum, H.; Pecoraro, V. L. Protein design: toward functional metalloenzymes. *Chem. Rev.* **2014**, *114*, 3495−3578.

(3) Hu, C.; Chan, S. I.; Sawyer, E. B.; Yu, Y.; Wang, J. Metalloprotein design using genetic code expansion. *Chem. Soc. Rev.* **2014**, *43*, 6498−6510.

(4) Poulos, T. L. Heme enzyme structure and function. *Chem. Rev.* **2014**, *114*, 3919−3962.

(5) Armstrong, C. T.; Watkins, D. W.; Anderson, J. L. R. Constructing man-made enzymes for oxygen activation. *Dalton Trans.* **2013**, *42*, 3136−3150.

(6) Reedy, C. J.; Gibney, B. R. Heme protein assemblies. *Chem. Rev.* **2004**, *104*, 617−649.

(7) Larsen, R. W.; Wojtas, L.; Perman, J.; Musselman, R. L.; Zaworotko, M. J.; Vetromile, C. M. Mimicking heme enzymes in the solid state: Metal-organic materials with selectively encapsulated heme. *J. Am. Chem. Soc.* **2011**, *133*, 10356−10359.

(8) Huang, S. S.; Gibney, B. R.; Stayrook, S. E.; Leslie Dutton, P.; Lewis, M. X-ray Structure of a Maquette Scaffold. *J. Mol. Biol.* **2003**, *326*, 1219−1225.

(9) Peacock, A. F. A. Incorporating metals into de novo proteins. *Curr. Opin. Chem. Biol.* **2013**, *17*, 934−939.

(10) Koder, R. L.; Anderson, J. L. R.; Solomon, L. A.; Reddy, K. S.; Moser, C. C.; Dutton, P. L. Design and engineering of an O_2 transport protein. *Nature* **2009**, *458*, 305−309.

(11) Farid, T. A.; Kodali, G.; Solomon, L. A.; Lichtenstein, B. R.; Sheehan, M. M.; Fry, B. A.; Bialas, C.; Ennist, N. M.; Siedlecki, J. A.; Zhao, Z.; et al. Elementary tetrahelical protein design for diverse oxidoreductase functions. *Nat. Chem. Biol.* **2013**, *9*, 826−833.

(12) Joh, N. H.; Wang, T.; Bhate, M. P.; Acharya, R.; Wu, Y.; Grabe, M.; Hong, M.; Grigoryan, G.; DeGrado, W. F. De novo design of a transmembrane Zn2+-transporting four-helix bundle. *Science* **2014**, *346*, 1520−1524.

(13) Faiella, M.; Andreozzi, C.; de Rosales, R. T. M.; Pavone, V.; Maglio, O.; Nastri, F.; DeGrado, W. F.; Lombardi, A. An artificial di-iron oxo-protein with phenol oxidase activity. *Nat. Chem. Biol.* **2009**, *5*, 882−884.

(14) Faiella, M.; Maglio, O.; Nastri, F.; Lombardi, A.; Lista, L.; Hagen, W. R.; Pavone, V. De novo design, synthesis and characterisation of MP3, a new catalytic four-helix bundle hemeprotein. *Chem. - Eur. J.* **2012**, *18*, 15960−15971.

(15) Song, W. J.; Tezcan, F. A. A designed supramolecular protein assembly with in vivo enzymatic activity. *Science* **2014**, *346*, 1525−1528.

(16) Weisman, S.; Haritos, V. S.; Church, J. S.; Huson, M. G.; Mudie, S. T.; Rodgers, A. J. W.; Dumsday, G. J.; Sutherland, T. D. Honeybee silk: recombinant protein production, assembly and fiber spinning. *Biomaterials* **2010**, *31*, 2695−2700.

(17) Vidal, G.; Blanchi, T.; Mieszawska, A. J.; Calabrese, R.; Rossi, C.; Vigneron, P.; Duval, J.-L.; Kaplan, D. L.; Egles, C. Enhanced cellular adhesion on titanium by silk functionalized with titanium binding and RGD peptides. *Acta Biomater.* **2013**, *9*, 4935−4943.

(18) Krishnaji, S. T.; Kaplan, D. L. Bioengineered chimeric spider silk-uranium binding proteins. *Macromol. Biosci.* **2013**, *13*, 256−264.

(19) Gomes, S. C.; Leonor, I. B.; Mano, J. F.; Reis, R. L.; Kaplan, D. L. Antimicrobial functionalized genetically engineered spider silk. *Biomaterials* **2011**, *32*, 4255−4266.

(20) Mayavan, S.; Dutta, N. K.; Choudhury, N. R.; Kim, M.; Elvin, C. M.; Hill, A. J. Self-organization, interfacial interaction and photophysical properties of gold nanoparticle complexes derived from resilin-mimetic fluorescent protein rec1-resilin. *Biomaterials* **2011**, *32*, 2786−2796.

DOI: 10.1021/acsbiomaterials.5b00239
ACS Biomater. Sci. Eng. 2015, 1, 1114−1120

(21) Balu, R.; Whittaker, J.; Dutta, N. K.; Elvin, C. M.; Choudhury, N. R. Multi-responsive biomaterials and nanobioconjugates from resilin-like protein polymers. *J. Mater. Chem. B* **2014**, *2*, 5936.
(22) Currie, H. A.; Deschaume, O.; Naik, R. R.; Perry, C. C.; Kaplan, D. L. Genetically engineered chimeric silk-silver binding proteins. *Adv. Funct. Mater.* **2011**, *21*, 2889−2895.
(23) Berggren, G.; Adamska, A.; Lambertz, C.; Simmons, T. R.; Esselborn, J.; Atta, M.; Gambarelli, S.; Mouesca, J.-M.; Reijerse, E.; Lubitz, W.; et al. Biomimetic assembly and activation of [FeFe]-hydrogenases. *Nature* **2013**, *499*, 66−69.
(24) Hepburn, H. R.; Kurstjens, S. P. The combs of honeybees as composite materials. *Apidologie* **1988**, *19*, 25−36.
(25) Sutherland, T. D.; Young, J. H.; Weisman, S.; Hayashi, C. Y.; Merritt, D. J. Insect silk: one name, many materials. *Annu. Rev. Entomol.* **2010**, *55*, 171−188.
(26) Sutherland, T. D.; Campbell, P. M.; Weisman, S.; Trueman, H. E.; Sriskantha, A.; Wanjura, W. J.; Haritos, V. S. A highly divergent gene cluster in honey bees encodes a novel silk family. *Genome Res.* **2006**, *16*, 1414−1421.
(27) Sutherland, T. D.; Church, J. S.; Hu, X.; Huson, M. G.; Kaplan, D. L.; Weisman, S. Single honeybee silk protein mimics properties of multi-protein silk. *PLoS One* **2011**, *6*, e16489.
(28) Poole, J.; Church, J. S.; Woodhead, A. L.; Huson, M. G.; Sriskantha, A.; Kyratzis, I. L.; Sutherland, T. D. Continuous production of flexible fibers from transgenically produced honeybee silk proteins. *Macromol. Biosci.* **2013**, *13*, 1321−1326.
(29) Wittmer, C. R.; Hu, X.; Gauthier, P.-C.; Weisman, S.; Kaplan, D. L.; Sutherland, T. D. Production, structure and in vitro degradation of electrospun honeybee silk nanofibers. *Acta Biomater.* **2011**, *7*, 3789−3795.
(30) Huson, M. G.; Church, J. S.; Poole, J. M.; Weisman, S.; Sriskantha, A.; Warden, A. C.; Campbell, P. M.; Ramshaw, J. a M.; Sutherland, T. D. Controlling the molecular structure and physical properties of artificial honeybee silk by heating or by immersion in solvents. *PLoS One* **2012**, *7*, e52308.
(31) Rapson, T. D.; Church, J. S.; Trueman, H. E.; Dacres, H.; Sutherland, T. D.; Trowell, S. C. Micromolar biosensing of nitric oxide using myoglobin immobilized in a synthetic silk film. *Biosens. Bioelectron.* **2014**, *62*, 214−220.
(32) Sutherland, T. D.; Trueman, H. E.; Walker, A. A.; Weisman, S.; Campbell, P. M.; Dong, Z.; Huson, M. G.; Woodhead, A. L.; Church, J. S. Convergently-evolved structural anomalies in the coiled coil domains of insect silk proteins. *J. Struct. Biol.* **2014**, *186*, 402−411.
(33) Zastrow, M. L.; Pecoraro, V. L. Designing functional metalloproteins: from structural to catalytic metal sites. *Coord. Chem. Rev.* **2013**, *257*, 2565−2588.
(34) Poulos, T. L. The role of the proximal ligand in heme enzymes. *JBIC, J. Biol. Inorg. Chem.* **1996**, *1*, 356−359.
(35) Esselborn, J.; Lambertz, C.; Adamska-Venkatesh, A.; Simmons, T.; Berggren, G.; Noth, J.; Siebel, J.; Hemschemeier, A.; Artero, V.; Reijerse, E.; et al. Spontaneous activation of [FeFe]-hydrogenases by an inorganic [2Fe] active site mimic. *Nat. Chem. Biol.* **2013**, *9*, 607−609.
(36) Bethel, R. D.; Darensbourg, M. Y. Bioinorganic chemistry: Enzymes activated by synthetic components. *Nature* **2013**, *499*, 40−41.
(37) Roy, S.; Nguyen, T.-A. D.; Gan, L.; Jones, A. K. Biomimetic peptide-based models of [FeFe]-hydrogenases: utilization of phosphine-containing peptides. *Dalton Trans.* **2015**, *44*, 14865.
(38) Dawson, J. Probing structure-function relations in heme-containing oxygenases and peroxidases. *Science* **1988**, *240*, 433−439.
(39) Antonini, E.; Brunori, M. *Hemoglobin and Myoglobin in Their Reactions with Ligands*; North-Holland: Amsterdam, The Netherlands, 1971.
(40) Singh, B. R.; DeOliveira, D. B.; Fu, F.-N.; Fuller, M. P. Fourier transform infrared analysis of amide III bands of proteins for the secondary structure estimation. In *Optics, Electro-Optics & Laser Applications in Science & Engineering*; Nafie, L. A., Mantsch, H. H., Eds.; International Society for Optics and Photonics: Bellingham, WA, 1993; pp 47−55.
(41) Susi, H.; Byler, D. Fourier Transform Infrared Spectroscopy in Protein Conformation Studies. In *Methods for Protein Analysis*; Cherry, J., Barford, R., Eds.; American Oil Chemists Society: Champaign, IL, 1988; pp 235−250.
(42) Spiro, T. G. Resonance Raman spectroscopy as a probe of heme protein structure and dynamics. *Adv. Protein Chem.* **1985**, *37*, 111−159.
(43) Nagai, M.; Yoneyama, Y.; Kitagawa, T. Characteristics in tyrosine coordinations of four hemoglobins M probed by resonance raman spectroscopy. *Biochemistry* **1989**, *28*, 2418−2422.
(44) Nagai, K.; Kagimoto, T.; Hayashi, A.; Taketa, F.; Kitagawa, T. Resonance raman studies of hemoglobins M: evidence for iron-tyrosine charge-transfer interactions in the abnormal subunits of Hb M Boston and Hb M Iwate. *Biochemistry* **1983**, *22*, 1305−1311.
(45) Li, H.; Poulos, T. L. Structural variation in heme enzymes: a comparative analysis of peroxidase and P450 crystal structures. *Structure* **1994**, *2*, 461−464.
(46) Ascoli, F.; Rossi Fanelli, M. R.; Antonini, E. Preparation and properties of apohemoglobin and reconstituted hemoglobins. *Methods Enzymol.* **1981**, *76*, 72−87.
(47) Adler, P. R.; Arora, R.; El Ghaouth, A.; Glenn, D. M.; Solar, J. M. Bioremediation of Phenolic Compounds from Water with Plant Root Surface Peroxidases. *J. Environ. Qual.* **1994**, *23*, 1113.
(48) Danner, D. J.; Brignac, P. J.; Arceneaux, D.; Patel, V. The oxidation of phenol and its reaction product by horseradish peroxidase and hydrogen peroxide. *Arch. Biochem. Biophys.* **1973**, *156*, 759−763.
(49) Nakamoto, S.; Machida, N. Phenol removal from aqueous solutions by peroxidase-catalyzed reaction using additives. *Water Res.* **1992**, *26*, 49−54.
(50) Lubitz, W.; Lendzian, F.; Bittl, R. Radicals, Radical Pairs and Triplet States in Photosynthesis. *Acc. Chem. Res.* **2002**, *35*, 313−320.
(51) Rio, Y.; Salomé Rodríguez-Morgade, M.; Torres, T. Modulating the electronic properties of porphyrinoids: a voyage from the violet to the infrared regions of the electromagnetic spectrum. *Org. Biomol. Chem.* **2008**, *6*, 1877−1894.
(52) Ludwig, M. L.; Matthews, R. G. Structure-based perspectives on B12-dependent enzymes. *Annu. Rev. Biochem.* **1997**, *66*, 269−313.
(53) Ragoussi, M.-E.; Ince, M.; Torres, T. Recent Advances in Phthalocyanine-Based Sensitizers for Dye-Sensitized Solar Cells. *Eur. J. Org. Chem.* **2013**, *2013*, 6475−6489.
(54) Ince, M.; Yum, J.-H.; Kim, Y.; Mathew, S.; Grätzel, M.; Torres, T.; Nazeeruddin, M. K. Molecular Engineering of Phthalocyanine Sensitizers for Dye-Sensitized Solar Cells. *J. Phys. Chem. C* **2014**, *118*, 17166−17170.
(55) Vicente, M. G. Porphyrin-based sensitizers in the detection and treatment of cancer: recent progress. *Curr. Med. Chem.: Anti-Cancer Agents* **2001**, *1*, 175−194.
(56) Rapson, T. D.; Dacres, H.; Trowell, S. C. Fluorescent nitric oxide detection using cobalt substituted myoglobin. *RSC Adv.* **2014**, *4*, 10269−10272.
(57) Zagal, J. H.; Griveau, S.; Silva, J. F.; Nyokong, T.; Bedioui, F. Metallophthalocyanine-based molecular materials as catalysts for electrochemical reactions. *Coord. Chem. Rev.* **2010**, *254*, 2755−2791.

DOI: 10.1021/acsbiomaterials.5b00239
ACS Biomater. Sci. Eng. 2015, 1, 1114−1120